Scientific Reports

https://doi.org/10.1038/s41598-026-50376-7

Article in Press

Sustainable adsorptive removal of eriochrome black T Dye using *Cladophora glomerata* biochar

Received: 19 November 2025

Accepted: 21 April 2026

Published online: 27 April 2026

Cite this article as: Aman F., Farooq U., Bibi K. *et al.* Sustainable adsorptive removal of eriochrome black T Dye using *Cladophora glomerata* biochar. *Sci Rep* (2026). https://doi.org/10.1038/s41598-026-50376-7

Fariha Aman, Umar Farooq, Khudeja Bibi, Mohd Abul Hasan, Sajid Ali, Syed Lal Badshah, Shabir Ahmad, Nawshad Muhammad, Sabiha Sultana, Muhammad Ilyas, Thiago Machado Silva Acioly & Alibek Ydyrys

Sustainable Adsorptive Removal of Eriochrome Black T Dye Using *Cladophora glomerata* Biochar

Fariha Aman[1], Umar Farooq[1], Khudeja Bibi[1], Mohd Abul Hasan[2], Sajid Ali[3], Syed Lal Badshah[1], Shabir Ahmad[1], Nawshad Muhammad[4], Sabiha Sultana[1*], Muhammad Ilyas[5], Thiago Machado da Silva Acioly[6], Alibek Ydyrys[7,8]

[1]Department of Chemistry, Islamia College Peshawar, Peshawar 25120, Khyber Pakhtunkhwa Pakistan. E-mails: farihaaman136@gmail.com (F. Aman), uf86654@gmail.com (U. Farooq), khankhadija299@gmail.com (K. Bibi), shahbiochemist@gmail.com (S.L. Badshah), shabir.ahmad@icp.edu.pk (S. Ahmad), sabiha@icp.edu.pk (S. Sultana)
[2]Department of Civil Engineering, College of Engineering, King Khalid University, Abhã, Kingdom of Saudi Arabia. E-mail: mohad@kku.edu.sa
[3]CAS Key Laboratory of Urban Pollutant Conversion, Institute of Urban Environment, Chinese Academy of Sciences, Xiamen 361021, China. E-mail: sajid@iue.ac.cn (S. Ali)
[4]Institute of basic medical science, Khyber medical university, Peshawar, Khyber Pakhtunkhwa Pakistan. E-mail: nawshad.ibms@kmu.edu.pk
[5]Department of Environmental Sciences, Faculty of Sciences, International Islamic University, Islamabad, 44000, Pakistan. E-mails: sirfilyas@yahoo.com
[6]Federal Institute of Education, Science and Technology of the Sertão Pernambucano (IFSertãoPE), Campus Floresta, Floresta, Pernambuco, 56400-000, Brazil. E-mail: tmsacioly@gmail.com
[7]Biomedical Research Centre, Al-Farabi Kazakh National University, Al-Farabi Ave. 71, 050040, Kazakhstan. E-mail: Alibek.ydyrys@kaznu.edu.kz
[8]Khoja Akhmet Yassawi International Kazakh-Turkish University, Turkistan, Sattarkhanov Ave. 29, 161200, Kazakhstan.

*This is corresponding author.

Abstract

Water contamination by synthetic dyes poses a serious threat to aquatic ecosystems and human health, thus urgently requiring cost-effective and sustainable remediation strategies. In this research work, *Cladophora glomerata* algae were pyrolyzed at a slow rate (10 °C/min) at 350 °C for two hours in order to produce high efficiency value-added biochar and were used for the removal of an azo dye called Eriochrome Black T (EBT) from water through adsorption. The adsorbent was characterized by using various physicochemical analyses and experimental techniques. According to proximate and EDS analysis, the chosen biochar is a rich source of nutrients, including Ca, K, Mg, and P as well as carbon (47.67 wt. %), oxygen (40.04 wt. %), and other elements. A higher yield of 67% means that less weight is lost during pyrolysis, which allows for the production of more amount of biochar. FTIR data show that Peaks at 3853 cm^{-1} and 2312 cm^{-1} in the spectra of biochar were linked to the stretching frequency of the OH group. The abundance of OH functional groups imparts a negative charge to the biochar, providing potential active sites for dye biosorption. SEM images identified diatoms on the algal surface, diatoms are a component of ash that are present in the biochar sample. The maximum dye uptake capacity (q_m) was 58.55625 mg/g at pH 2, 60 ppm dye concentration, 0.1g biochar dosage, and 120 minutes of equilibrium time at room temperature. The adsorption followed the Langmuir isotherm model (R^2 = 0.9711) and pseudo-second-order kinetics (R^2 = 0.9992, K_2 = 0.006139 g/mg.min, q_t = 58.47953 mg/g). Thermodynamic analysis shows that the adsorption process is endothermic ($\Delta H°$ = 6.92621 KJ/mol^{-1}) and spontaneous ($\Delta G° <$ 0). These results demonstrate that *Cladophora glomerata*-derived biochar is a highly efficient and sustainable adsorbent for removing synthetic dyes from water.

Keywords: Microalgal biomass; azo dye contamination; low-cost adsorbent; adsorption isotherms; kinetic modeling; thermodynamic parameters; wastewater remediation

Introduction

Water is one of the most essential resources for all living organisms, yet it is frequently contaminated by hazardous pollutants such as polycyclic aromatic hydrocarbons (PAHs), heavy metals, dyes, pharmaceuticals, pesticides, and herbicides[1,2,3,4]. The toxic impacts of dyes, one of the most widespread classes of organic contaminants, on aquatic organisms and humans are well documented[5]. The increasing concentrations of toxic pollutants in aquatic environments originate from natural, industrial, agricultural, and domestic activities, including volcanic eruptions, industrial expansion, urbanization, direct discharge of industrial effluents, sewage disposal, inappropriate solid-waste management, herbicide runoff, and radioactive emissions[6,7,8,9]. Among the industries employing dyes, the textile sector is the largest global consumer, using dyes extensively for fiber coloration[10].

Industrial growth represents a major source of water contamination. Sectors such as metal processing, paper manufacturing, mining, battery production, textiles, and leather generate large volumes of wastewater rich in harmful chemicals, which deeply affect aquatic ecosystems. Of the pollutants released, dyes and heavy metals have received particular attention due to their persistence and long-term toxicity to humans, animals, and plants[11,12,13,14]. Moreover, the complex molecular structure of synthetic dyes and the non-biodegradable nature of many metal ions make their removal through conventional treatment methods particularly challenging, thus reinforcing the need for alternative, low-cost, and environmentally sustainable remediation technologies.

The global textile industry is valued at over $1 trillion USD, contributes 7% of worldwide exports, and provides employment to 35

million people[15]. However, it is also a significant contributor to environmental degradation. Textile effluents, typically characterized by high salinity, high chemical oxygen demand, and intense coloration, adversely affect aquatic life and pose health risks to humans and animals[15,16,17]. Synthetic dyes frequently exhibit acute and chronic toxicity, including dermatitis, occupational asthma, rhinitis, and allergic reactions[15]. Many dyes are also mutagenic and carcinogenic, contributing to liver, kidney, and bladder cancers among exposed populations[18]. For example, erythrosine, a xanthene dye, is known for its neurotoxic, carcinogenic, and DNA-damaging effects[19]. Due to the limitations of conventional treatment methods, advanced alternatives such as bioremediation and adsorption using biochar are increasingly needed to prevent further contamination by carcinogenic and mutagenic compounds[15].

Dyes are organic compounds that impart color and are typically water-soluble, unlike insoluble pigments[20]. Eriochrome Black T (EBT) is an anionic azo dye widely used in complexometric titrations and in coloring silk, wool, and nylon[21]. It is highly resistant to aerobic biological degradation, making its removal from water challenging[22]. EBT forms red-colored complexes with calcium, magnesium, and other metal ions[23]. Azo dyes, of which over 100.000 commercial varieties exist, are prevalent in textile, leather, food, paint, and pigment industries. Their aromatic structures confer high stability and resistance to biodegradation, reducing light penetration in water, suppressing photosynthesis, and promoting bacterial growth[24]. Due to their respiratory toxicity, mutagenicity, teratogenicity, and carcinogenicity, azo dyes pose severe risks to aquatic species and humans. Excessive EBT discharge further reduces water reoxygenation capacity and impairs photosynthesis in phytoplankton and aquatic vegetation[25].

Among available treatment technologies, adsorption stands out due to its affordability, high efficiency, and minimal operational requirements[15,26]. Various low-cost adsorbents have been tested for EBT removal, such as tea

waste[22], rice-hull activated carbon[27], Persea species vegetable waste[28], and peanut shells[29]. However, the demand for effective, low-cost alternatives remains. Biochar has emerged as a promising adsorbent due to its high adsorption capacity, 10 to 1000 times greater than many carbon-based materials[30], and its ability to remove a broad spectrum of contaminants, including agrochemicals, antibiotics, industrial chemicals, aromatic dyes, PAHs, and volatile organic compounds[31].

Biochar has gained increasing attention as an environmentally friendly and highly versatile adsorbent, characterized by its high carbon content, substantial cation-exchange capacity, large surface area, and porous structure[32]. In recent years, research on its applications in wastewater treatment has expanded rapidly[33,34]. Owing to these adsorption properties, biochar has proven effective for removing hazardous colorants and other pollutants. A particularly promising strategy involves producing biochar, or activated carbon, from algal biomass residues generated during biodiesel production[35]. Activated carbon adsorption remains one of the most efficient techniques for dye removal[27], and the development of advanced biochar materials is increasingly viewed as essential for the effective removal of EBT[25].

Algal-derived biochar, as a sustainable adsorbent, is increasingly being used to remove dyes and heavy metals from wastewater. However, research on the adsorption of anionic dyes such as EBT by green algae (*Cladophora glomerata*) biochar is limited, and therefore, its adsorption performance and optimal conditions remain unclear. The main objectives of this research are to investigate the use of *Cladophora glomerata* biochar as a non-conventional and low-cost adsorbent for removing EBT from wastewater. Biochar was synthesized from *Cladophora glomerata* through slow pyrolysis, and adsorption parameters, including contact time, adsorbent dosage, initial dye concentration, and pH were evaluated. Equilibrium data were analyzed using the Langmuir and the Freundlich isotherm models, while adsorption kinetics were examined using pseudo-

first-order and pseudo-second-order models. This work contributes to the growing interest in sustainable and bio-based adsorbents by exploring algal-derived biochar, a biomass source that remains less studied compared with conventional agricultural and lignocellulosic residues.

The innovation of this study lies in combining the resource utilization of algal waste with adsorption models, providing a new method for optimizing the use of *Cladophora glomerata* biochar to remove anionic dyes (such as EBT). This work uniquely combines underutilized biomass precursors, systematic evaluation of adsorption performance, and application in related textile dyes, highlighting the innovativeness of this research in the field of advanced wastewater treatment materials. Furthermore, this study supports UN Sustainable Development Goal 6 (Clean Water and Sanitation) by providing an easy-to-operate, environmentally friendly, and resource-efficient method to enhance dye removal from contaminated water. The resource utilization of algal residue also aligns with circular economy principles, promotes sustainable waste management, and demonstrates the potential for developing low cost treatment solutions for areas severely affected by textile wastewater.

Materials and methods

Chemical reagents

All chemicals and reagents used in this study were of analytical grade. Sodium hydroxide (NaOH, 99%; BDH), hydrochloric acid (HCl, 37%; Sigma-Aldrich, Chemei GmbH, Germany), and Eriochrome Black T dye ($C_{20}H_{12}N_3NaO_7S$; Lot: 5851478545; EYER, China) were used as received. The *Cladophora glomerata* biochar was produced from algal biomass collected from the Swat River and its tributaries (Pakistan). Distilled water, prepared in the laboratory, was used for all experiments.

Preparation of solutions

A 0.1 M NaOH solution was prepared by dissolving 1 g of NaOH in distilled water and diluting the solution to a final volume of 250 mL. Similarly, 0.1 M HCl was prepared by adding 2.075 mL of concentrated HCl to distilled water and diluting to 250 mL. For the dye stock solution, 1 g of EBT was dissolved in 1000 mL of distilled water to obtain a concentration of 1000 mg/L (1000 ppm). Working solutions of 10, 20, 30, 40, 50, 60, and 70 ppm were prepared from the stock by successive dilutions using the equation shown in Equation (1) (Table S1). The absorbance of each solution was measured using a UV–Visible spectrophotometer at λmax = 530 nm, and a standard calibration curve was plotted for subsequent adsorption calculations.

$$C_1V_1=C_2V_2 \quad (1)$$

Where: C_1= concentration of stock solution (ppm); V_1= volume of stock solution required (mL); C_2= desired concentration (ppm); V_2= final volume of diluted solution (mL).

Collection and preparation of adsorbent

Collection of algae

Freshwater macroalgae of the species *Cladophora glomerata* were collected from the Swat River and its tributaries in Charsadda, Khyber Pakhtunkhwa, Pakistan. The species was identified by a plant taxonomist from the Department of Botany at Islamia College Peshawar. The collected algae were initially rinsed with tap water and subsequently washed three times with distilled water to remove sand and dust particles. After washing, the material was sun-dried outdoors. Once completely dried, the algae were ground into a fine powder using a homemade grinder. The powdered biomass was stored in airtight containers for further experimental work.

Preparation of adsorbent

Pyrolysis of fresh water macroalgae

Biochar was produced through the pyrolysis of *Cladophora glomerata* biomass using an electrically heated Carbolite furnace. To ensure an inert atmosphere, the furnace chamber was purged with nitrogen gas prior to each run. Slow pyrolysis was employed, characterized by a low heating rate and extended residence time, allowing maximal thermal exposure of the biomass. Approximately 3.0 g of dried algal powder was weighed, placed into a crucible, and inserted horizontally into the furnace. Pyrolysis was performed at a final temperature of 350 °C, a heating rate of 10 °C/min, and a residence time of 2 hours. After completion, the samples were allowed to cool naturally to room temperature. The biochar yield (%) was calculated following cooling.

Yield of biochar

After weighing the produced biochar, the yield percentage (Y) was calculated using Equation (2), which quantifies the proportion of solid product remaining and serves as a key indicator of pyrolysis efficiency and feedstock characteristics.

$$\% Y = \frac{\text{Mass after pyrolysis}}{\text{Mass before pyrolysis}} \times 100 \qquad (2)$$

Meshing of biochar

To obtain a homogeneous sample, the size distribution was performed using a meshing sieving machine (Model AS 200, Retsch, Germany) with the following mesh sizes: 500 µm, 250 µm, 125 µm, 63 µm, 45 µm, and <45 µm. The selected mesh fraction was 146 µm, which was then stored in airtight polyethylene bags for further analysis.

Characterization of adsorbent

The concentration of EBT dye in solution before and after adsorption was quantified spectrophotometrically at a wavelength of 530 nm. The physicochemical characteristics of *Cladophora glomerata* biochar were evaluated using several analytical techniques. Moisture content, volatile matter, ash content, and fixed carbon were determined following ASTM standard methods (ASTM, 1998; ASTM, 2009). Elemental composition was assessed using an Energy Dispersive Spectrometer (EDS) to determine the weight percentage of surface chemical constituents. Scanning Electron Microscopy (SEM) was employed to examine the surface morphology of the biochar. Functional groups present on the adsorbent surface were identified through FT-IR analysis. In addition, X-ray diffraction (XRD) analysis was conducted to determine the crystalline phases in the biochar.

Batch adsorption studies

Batch adsorption experiments were carried out using EBT dye as the adsorbate to evaluate the potential of the algal biochar for water treatment applications. To determine the percentage removal (% removal) and the amount of dye adsorbed per gram of adsorbent (q_e), the following parameters were investigated: 1. Initial dye concentration; 2. Adsorbent

dosage; 3. Contact time; 4. pH. All adsorption experiments were repeated three times, and the reported results represent the average value.

Effect of initial dye concentration

To determine the optimum initial concentration of EBT dye, solutions of 10, 20, 30, 40, 50, 60, and 70 ppm were prepared in 100 mL of distilled water. The pH of the solutions was adjusted to 2 by adding either 0.1 M HCl or 0.1 M NaOH. An amount of 0.1 g of biochar was added to each solution, which was then shaken at 150 rpm for 120 min at ambient temperature. After shaking, the solutions were filtered, and the absorbance of the filtrate was measured at the λmax of 530 nm using a UV-Visible spectrophotometer. The data were plotted as initial dye concentration (ppm) versus q_e and % adsorption to determine the optimal initial dye concentration.

Effect of adsorbent dosage

To determine the optimum adsorbent dosage, experiments were conducted using a 60 ppm EBT solution and varying amounts of biochar: 0.05, 0.1, 0.15, 0.2, 0.25, and 0.3 g. The pH of the solution was adjusted to 2 using either 0.1 M HCl or 0.1 M NaOH. All solutions were shaken at 150 rpm for 120 min at ambient temperature. After shaking, the solutions were filtered, and the absorbance of the filtrate was recorded at 530 nm. Data were plotted as adsorbent dosage (g) versus q_e and % adsorption to determine the optimum dosage.

Effect of contact time

To determine the optimum contact time, experiments were performed using a 60 ppm EBT solution at various time intervals: 0, 30, 60, 90, 120, 150, and 180 min. The pH of the solutions was adjusted to 2 using either 0.1 M HCl or 0.1 M NaOH. An amount of 0.1 g of biochar was added to each solution, which was then shaken at 150 rpm at ambient temperature. After shaking,

the solutions were filtered, and the absorbance of the filtrate was measured at 530 nm. Data were plotted as contact time (min) versus q_e and % adsorption to identify the optimum contact time.

Effect of pH

To determine the optimum pH value, experiments were conducted using a 60 ppm EBT dye solution at different pH levels: 1, 2, 3, 4, 5, 6, and 7. The pH of each solution was adjusted to the desired value by adding either 0.1 M HCl or 0.1 M NaOH. A 0.1 g portion of biochar was added to each solution, which was then shaken at 150 rpm for 120 min at ambient temperature. After shaking, the solutions were filtered, and the absorbance of the filtrate was measured at the λmax of 530 nm using a UV/Visible spectrophotometer.

$$\% \text{ Removal capacity} = \left[\frac{C_o - C_e}{C_o}\right] \times 100 \quad (3)$$

Where: C_o = initial dye concentration (mg/L); C_e = concentration of EBT dye at equilibrium (mg/L). The amount of dye adsorbed per unit mass of adsorbent at equilibrium, q_e (mg/g), was computed using Equation (4):

$$q_e = \left[\frac{C_o - C_e}{W}\right] \times V \quad (4)$$

Where: C_e = concentration of EBT dye at equilibrium (mg/L); C_o = concentration of EBT dye remaining in solution at equilibrium (mg/L); V = final volume of solution (L); W = adsorbent mass (g)[22].

Statistical analysis

All adsorption experiments were performed in triplicate to ensure reproducibility, and the results are expressed as mean ± standard deviation. Error bars representing standard deviation have been included in the relevant figures. The goodness-of-fit of adsorption isotherm models was evaluated using the coefficient of determination (R^2), chi-square (χ^2), and root mean square error (RMSE) values to assess model accuracy and

reliability. These statistical parameters were used to support the selection of the most appropriate isotherm model and to validate the experimental data.

Results and discussion

Characterization of the adsorbent

To evaluate the physicochemical properties of the biochar, several characterization methods were performed. Moisture, volatile matter, ash, and fixed carbon contents were quantified through proximate analysis. Elemental composition was assessed using Energy Dispersive Spectroscopy (EDS) to determine the percentage weight of surface chemical elements. The surface morphology and internal structure of the biochar were examined through scanning electron microscopy (SEM), while Fourier Transform Infrared Spectroscopy (FTIR) identified the functional groups involved in EBT dye adsorption. These characteristics directly influence the adsorption performance and potential environmental applications of algal biochar. Studies in the literature similarly report that biochars produced from biowaste present porous structures, high surface area, and abundant functional groups, supporting their application in removing hazardous contaminants from wastewater [36,37,38,39,40].

Proximate analysis of biochar

Cladophora glomerata is an aquatic biomass rich in mineral constituents and volatile organic compounds. The produced biochar exhibited a low moisture content of 6% and a high ash content of 42% (Table S2). This elevated ash content aligns with values commonly reported for algal-derived biochars. The high volatile matter content is attributed not only to the relatively low pyrolysis temperature but also to the biochemical composition of algae, which consists mainly of cellulose, hemicellulose, and proteins[41]. During pyrolysis, the decomposition of hemicellulose and cellulose generates substantial amounts of light hydrocarbons and oxygenated compounds (e.g., acids, ketones), along with carbon monoxide and carbon dioxide[42]. The biochar yield of 67% indicates limited mass loss during pyrolysis, allowing for the production of a comparatively higher amount of biochar, consistent with previous studies[43].

Fourier-transform infrared spectroscopy (FTIR)

FTIR analysis was conducted to identify the surface functional groups involved in adsorption, as these groups play a key role in biosorption mechanisms[37]. The FTIR spectrum of *Cladophora glomerata* biochar (Figure 1) revealed the presence of hydroxyl, phenolic, aldehydic, ketonic, and carboxylic acidic groups, which originate from the macromolecular components of macroalgae and serve as active binding sites for adsorption[44]. The most prominent absorption bands are located in the fingerprint region (1600-400 cm^{-1}). Two notable peaks at 3853 cm^{-1} and 2312 cm^{-1} correspond to O-H stretching vibrations, consistent with the abundance of hydroxyl groups. These OH-rich surfaces result in an overall negative charge, enhancing electrostatic interactions with positively charged species.

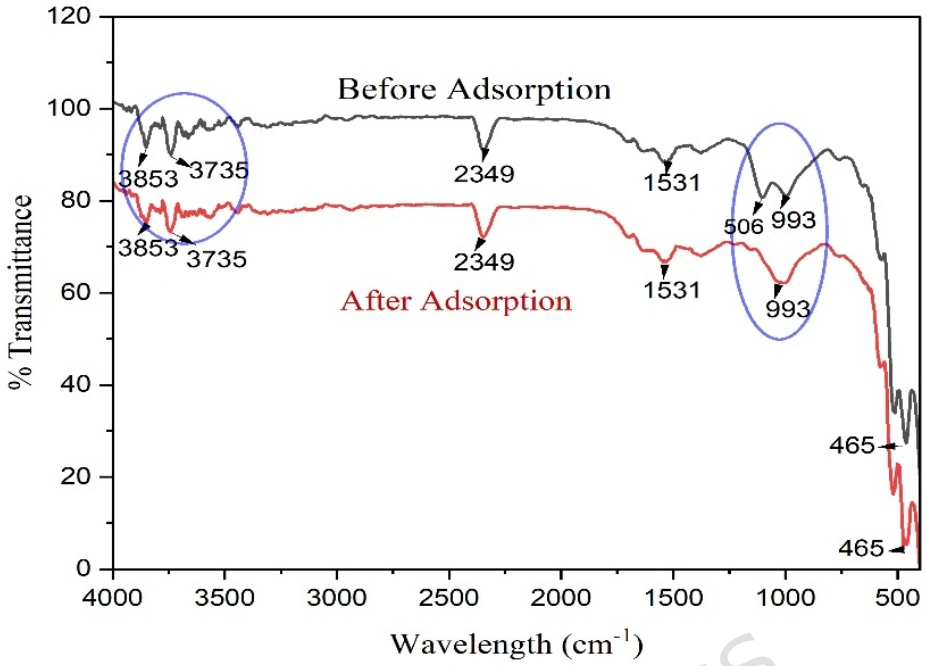

Figure 1. FTIR spectrum of Cladophora *glomerata* biochar before and after adsorption.

This investigation did not find any significant peaks in the 3730 to 2970 cm^{-1} region, although according to the study by Michalak et al.[36] this region usually contains weak OH signals and bands associated with C-H stretching vibrations in aliphatic CH_2 and CH groups. These OH and C-H functional groups are crucial because they impart a negative surface charge to biochar and provide potential active sites for dye adsorption. Characteristic mid-infrared absorption peaks include: 1531 cm^{-1} attributed to aromatic C=C and C=N stretching vibrations, enhancing π-π interactions with aromatic dye molecules; 1401 cm^{-1} associated with CH_2 bending vibrations, contributing to structural stability; 993 cm^{-1} a strong absorption band corresponding to Si-O-Si deformation vibrations, indicating a high silica content in algal-derived biochar, which can participate in adsorption; and ~617 cm^{-1} attributed to Fe-O bond vibrations, potentially promoting coordination with dye molecules. Overall, these functional groups, especially carboxyl, hydroxyl, and silanol groups, play a key role in

determining the adsorption capacity of biochar through ion exchange, complexation, and electrostatic interactions with dyes and metal ions[37,45,46].

Energy dispersive spectroscopy (EDS)

Energy Dispersive Spectroscopy (EDS) was used to evaluate the elemental composition of the biochar surface and to confirm the presence of mineral-rich ash components derived from the macroalgal biomass (Figure 2a-b). In algae-derived biochars, the ash fraction typically contains metals such as calcium, potassium, magnesium, sodium, aluminum, and iron, as well as non-metals including silicon and sulfur. These elements originate from the mineral constituents naturally accumulated by macroalgae. Consistent with previous studies, the biochar exhibited a high proportion of carbon (C) and oxygen (O), which are characteristic of biomass-derived chars[47]. Macroalgal biochars are also known to contain substantial amounts of Ca, K, Mg, and P, reflecting their nutrient-rich composition[48]. Before adsorption, the weight percentages of carbon and oxygen were 47.67 wt.% and 40.04 wt.%, respectively. After adsorption, these values changed to 45.01 wt.% (C) and 43.43 wt.% (O), as shown in Table S3. Variations in carbon content among different biochars commonly arise from differences in biomass type, moisture content, pyrolysis temperature, and residence time[39,49].

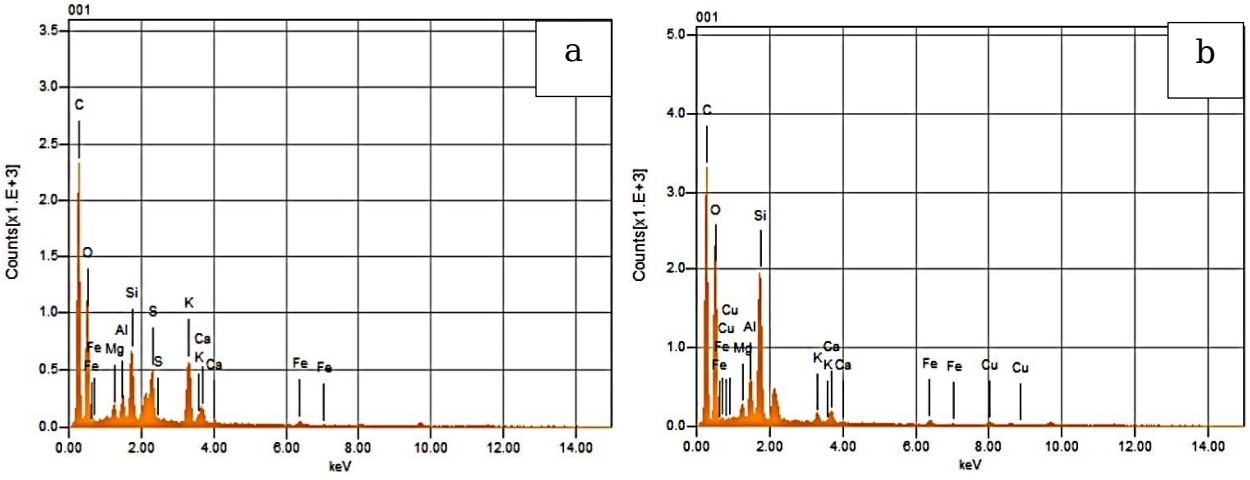

Figure 2. Comparison of EDS spectra of *Cladophora glomerata* biochar before (a) and after (b) adsorption.

Scanning electron microscope (SEM)

SEM was employed to examine the morphology and microstructural characteristics of the biochar samples. This technique is widely applied in the characterization of algal-derived biochars, as it provides detailed visualization of surface features and porosity[37,38]. Understanding these morphological attributes is essential, since the surface architecture directly influences adsorption performance by affecting surface area, pore distribution, and the accessibility of active binding sites.

(a) **(b)**

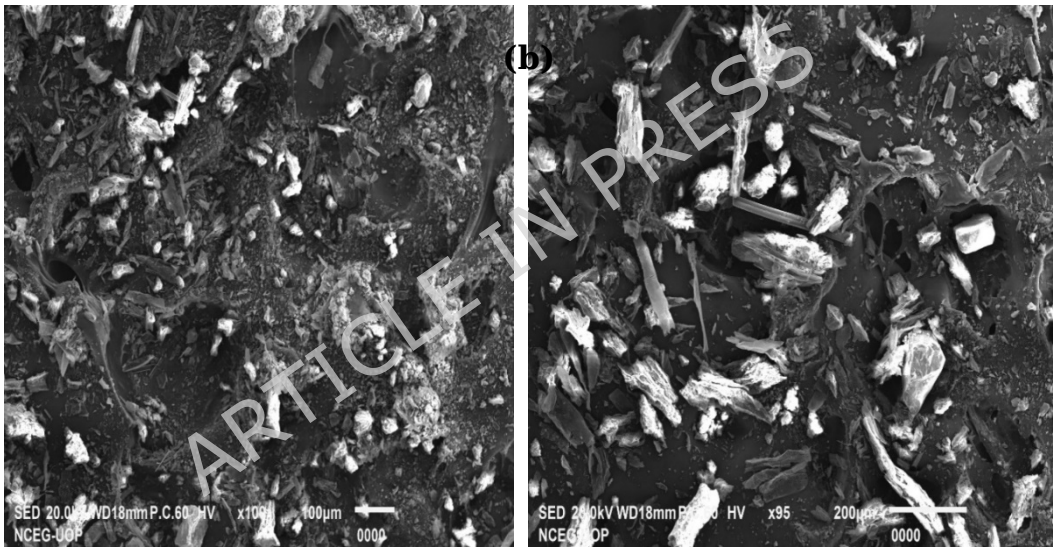

Figure 3. Comparative SEM micrographs of *Cladophora glomerata* biochar before (a) and after (b) adsorption.

The presence of diatoms in the biomass sample accounts for the silica-based structures clearly visible on the surface of the material (Figure 2). These microorganisms remain attached to the algal surface and are typically associated with favorable environmental conditions that promote their growth. As reported by Greenwood et al.[50], diatoms can be observed on macroalgal surfaces, and several taxa may be recognizable in SEM

micrographs (Figure 3 a-b). Because diatom cell walls consist mainly of hydrated silica (silicon oxide), their contribution to the ash fraction becomes more pronounced at higher pyrolysis temperatures, which enhances the concentration of inorganic residues in the resulting biochar. In addition, the pores and curvatures observed on the biochar surface appear more developed due to the release of low-molecular-weight gaseous compounds during pyrolysis, which may interact with and restructure the carbon matrix. Increasing temperature and ash content can also promote particle agglomeration, as previously noted by Liu et al.[51], resulting in denser structural domains within the biochar.

X-ray diffraction analysis

The crystalline and amorphous phases of *Cladophora glomerata* biochar were examined using X-ray diffraction (XRD). As shown in Figure 4, broad Bragg reflections were detected at approximately $2\theta \approx 20–30°$, which are characteristic of amorphous carbon and indicate the presence of disordered carbonaceous structures and microporosity within the biochar matrix. The diffractogram also exhibited additional sharp peaks, associated with inorganic mineral impurities, predominantly metal salts retained from the original algal biomass. The most intense peaks were attributed to crystalline phases of calcium carbonate ($CaCO_3$) and silica (SiO_2), in agreement with previous findings for algal-derived biochars[52]. The occurrence of these mineral constituents is consistent with the high ash content observed in the proximate analysis, reflecting the naturally mineral-rich composition of macroalgae.

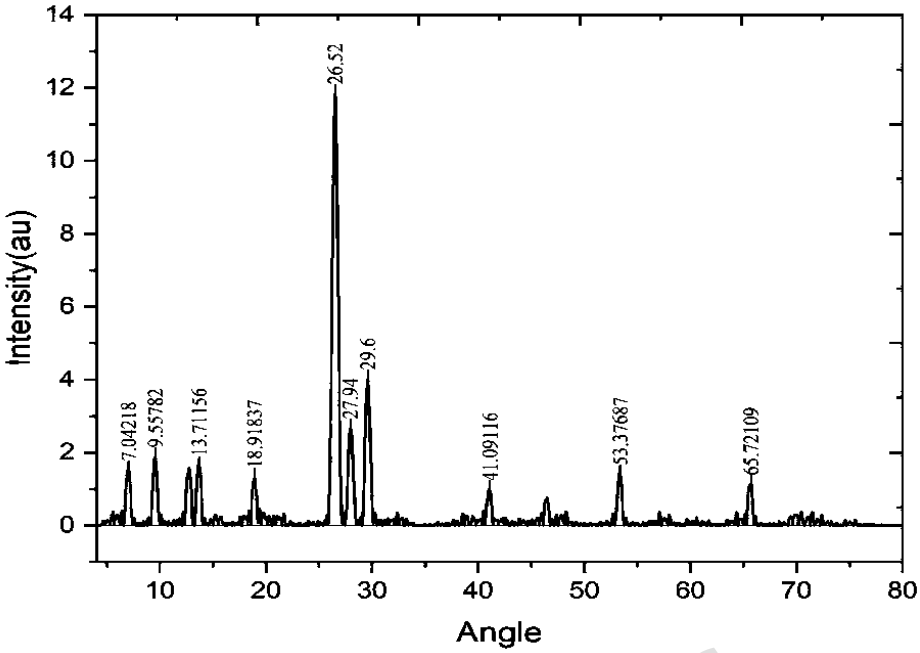

Figure 4. XRD profile of Cladophora *glomerata* biochar.

Thermogravimetric and differential thermogravimetric analysis (TGA/DTA)

Figure 5 shows the thermogravimetric (TGA) and differential thermogravimetric (DTA) curves obtained for 5.221 mg of *Cladophora glomerata* biochar. The analysis was carried out from 31 to 800 °C at a constant heating rate of 10 °C min^{-1} under an inert nitrogen atmosphere (20 mL min^{-1}). The thermal decomposition profile indicates a progressive mass loss associated with the degradation of organic constituents and the transformation of inorganic fractions. The initial mass loss of 1.375% between 50 and 150 °C corresponds to the evaporation of moisture and light extractive compounds. The most significant degradation event occurs between 220 and 550 °C, with an approximate mass loss of 27%, representing the active pyrolysis region, during which the major biopolymer components of the algal biomass decompose. The first DTA peak within this region is typically associated with carbohydrate degradation (200–300 °C), while the second peak corresponds to the thermal breakdown of proteins

(300–390 °C), consistent with the reported pyrolysis behavior of macroalgae-based biomaterials.

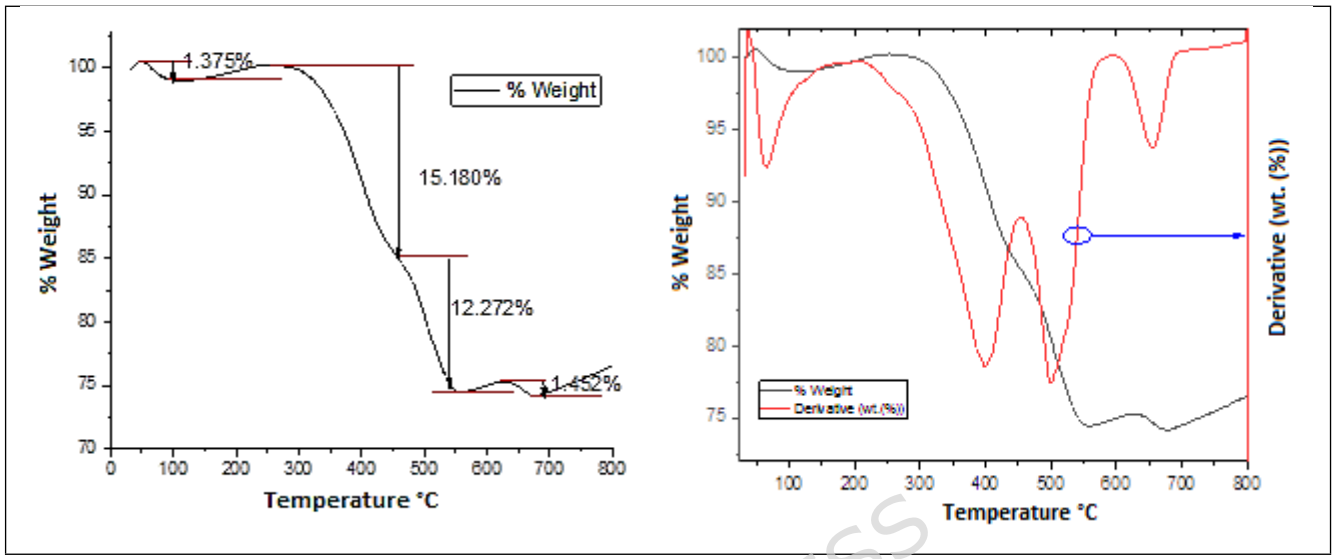

Figure 5. Thermogravimetric (TGA/DTA) curves of *Cladophora glomerata* biochar.

Above 500 °C, the biochar exhibits a slower and continuous mass loss, attributed mainly to the decomposition and restructuring of inorganic constituents, characterizing the passive pyrolysis region. Similar high-temperature degradation of mineral phases in macroalgal biochar has been reported in previous studies[53]. According to the TGA curve, thermal decomposition is nearly complete at approximately 600 °C, indicating the formation of a more thermally stable carbonaceous material. Therefore, the resulting thermally stable carbon matrix reinforces the potential of *Cladophora glomerata* biochar as a robust and efficient adsorbent for wastewater treatment applications.

Batch adsorption studies

The effects of different operational parameters on the removal of EBT dye were assessed through batch adsorption experiments. The study evaluated the influence of initial dye concentration, adsorbent dosage, solution pH, and contact time on the adsorption performance[22]. Biochar derived from *Cladophora glomerata* was employed as the adsorbent for EBT removal. The optimization of these conditions provides insights into the potential application of biochar as an efficient and sustainable adsorbent for dye-contaminated wastewater.

Standard calibration curve for EBT

A standard calibration curve was established to determine EBT concentrations before and after adsorption. A series of solutions with concentrations of 10, 20, 30, 40, 50, 60, and 70 ppm were prepared in distilled water due to the complete solubility of the dye in this medium (Figure S1). The absorbance values for each standard solution were measured using a UV–Visible spectrophotometer at a maximum wavelength (λmax) of 530 nm (Table S4). The dye exhibited a linear response across the investigated concentration range, producing a regression equation of: $y = 0.016x$ with a high correlation coefficient ($R^2 = 0.9716$), confirming the reliability of the calibration. This calibration curve was subsequently used to determine the EBT concentrations in the solutions before and after equilibrium adsorption.

Determination of the point of zero charge (PZC)

The PZC of *Cladophora glomerata* biochar was determined in a 60 ppm solution over an initial pH range of 1 to 7. The pH of each solution was adjusted using either 0.1 M HCl or 0.1 M NaOH. Subsequently, 0.1 g of the biochar adsorbent was added to each flask. The suspensions were agitated at 150 rpm for 120 minutes at room temperature. After shaking, the mixtures were filtered, and the final pH values (pHf) of the supernatants

were recorded. The difference between the initial and final pH values was calculated as ΔpH = (pHi – pHf). A plot of ΔpH versus pHi was then constructed, and the PZC was identified at the intersection point where ΔpH = 0. The PZC of *Cladophora glomerata* biochar was determined to be 5.9, as shown in Figure 6.

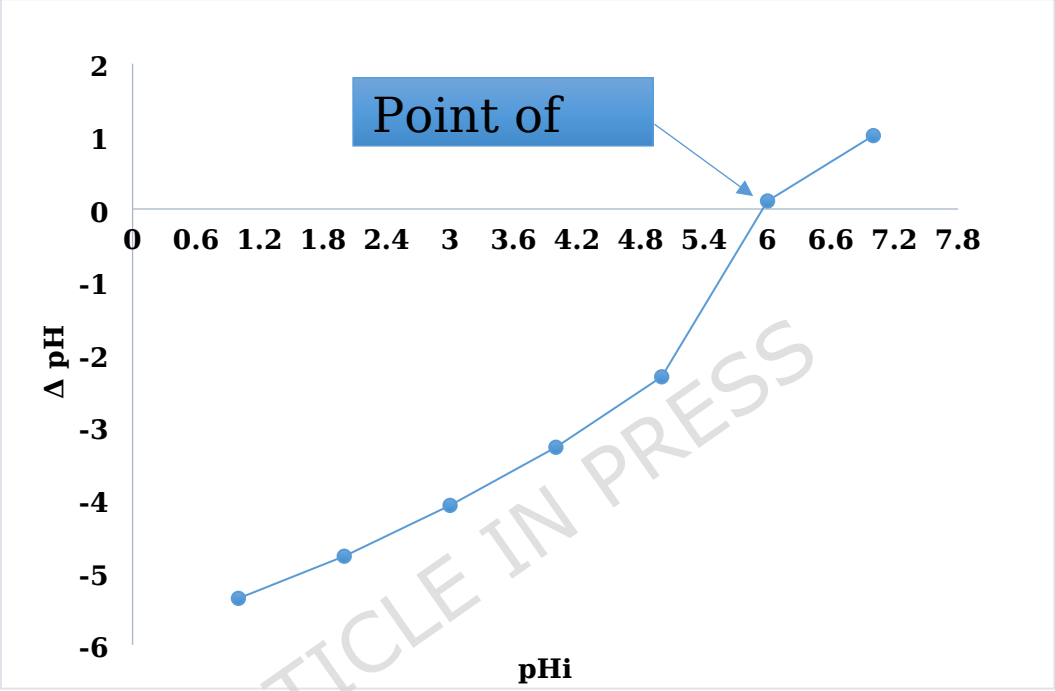

Figure 6. PZC of Cladophora *glomerata* biochar.

The concentration of H^+ ions in the solution increases when the pH falls below the PZC, causing the surface of *Cladophora glomerata* biochar to adsorb H^+ ions and acquire positive charges. This positively charged surface promotes strong electrostatic interactions with the negatively charged EBT molecules, resulting in maximum dye adsorption at low pH values. Conversely, at pH values above the PZC, the biochar surface becomes negatively charged, leading to electrostatic repulsion that hinders EBT adsorption. These findings emphasize the critical role of solution pH in

optimizing the removal of EBT using this biochar, with pH values below 5.9 identified as optimal for adsorption.

Effect of initial concentration

A series of experiments was performed to evaluate the impact of different initial concentrations of EBT dye (10, 20, 30, 40, 50, 60, and 70 ppm) on the adsorption efficiency of *Cladophora glomerata* biochar. The experiments were conducted under controlled conditions: adsorbent dosage of 0.1 g, solution pH 2, contact time of 120 min, and agitation speed of 150 rpm at room temperature. The results indicate that the uptake of EBT increases with the initial dye concentration due to a greater driving force and more dye molecules interacting with the available active sites on the biochar surface. Both the percentage removal and the adsorption capacity (q_e) increased with dye concentration and reached saturation at 60 ppm[54]. Therefore, an initial concentration of 60 ppm, corresponding to 50.10% removal, was selected for subsequent batch experiments (Table 1).

Table 1. Effect of initial concentration on amount adsorbed.

S. No	Concentration (ppm)	Q_e (mg/g)	% R
1	10	2.3125	23.125
2	20	6.6875	33.4375
3	30	11.9375	39.79166
4	40	18.4375	46.093
5	50	23.875	47.75
6	60	30.0625	50.104
7	70	35.9375	51.339

Effect of algal biochar dosage

The dosage of the adsorbent is a crucial factor that significantly affects sorption capacity[54,55]. Different amounts of biochar (0.05, 0.1, 0.15,

0.2, 0.25, and 0.3 g) were added to study this effect. Batch experiments were conducted using an initial EBT dye concentration of 60 ppm at pH 2, 150 rpm agitation, and 25°C. The equilibrium of *Cladophora glomerata* biochar was reached after 120 minutes. As shown in Table 2, increasing the biochar dosage from 0.05 g to 0.1 g led to a rise in percentage dye removal from 89.47916% to 89.79166%. This increase indicates that a higher biochar dosage provides more effective adsorption sites, promoting stronger interactions between EBT and the biochar surface. Therefore, the increase in surface area and the number of active sites improves the overall adsorption efficiency of EBT dyes. However, because the same amount of EBT is dispersed on a larger mass of adsorbent, the q_t per unit mass of biochar decreases from 107.375 mg/g to 53.875 mg/g. The relatively small increase in removal rate suggests that beyond a certain dosage, additional biochar contributes little to further dye adsorption, possibly due to site saturation or aggregation effects[28]. The highest dye removal was observed at 0.1 g of biochar. The corresponding dye uptake capacity (q_e) at different biochar dosages is presented in Table 2. The maximum q_e of 53.875 mg/g was achieved at 0.1 g of biochar, indicating the optimal adsorbent dosage for effective EBT removal.

Table 2. Effect of Cladophora *glomerata* biochar dosage on adsorption.

S. No	Concentration (ppm)	Dosage (g)	Q_e(mg/g)	% R
1	60	0.05	107.375	89.47916
2	60	0.1	53.875	89.79166
3	60	0.15	33.57083	83.92708
4	60	0.2	22.40625	74.688
5	60	0.25	15.575	64.89583
6	60	0.3	10.5	52.5

Effect of pH

The acidity or alkalinity of the solution strongly influences the dissociation of adsorption sites and, consequently, the adsorption efficiency of EBT dye. The effect of pH was investigated using 0.1 g of adsorbent, an initial dye concentration of 60 ppm, and a contact time of 120 min at 150 rpm. The results are summarized in Table 3. As shown in Table 3, the removal percentage decreased from 97.59% to 23.71% as the pH increased from 2 to 7. These results indicate that the amount of dye adsorbed increases under acidic conditions. The maximum adsorption at pH 2 can be attributed to the higher concentration of H^+ ions, which compete with the anionic groups of the dye for adsorption sites. At higher pH values, the presence of OH^- ions and the anionic groups on the dye causes electrostatic repulsion, reducing adsorption efficiency. Table 3 shows the trend of the amount of EBT dye adsorbed (mg/g) with changing pH. The adsorption capacity is highest at pH 2 and decreases steadily as pH increases, further confirming that acidic conditions favor adsorption due to enhanced electrostatic attraction between the cationic sites on the adsorbent and the anionic dye molecules.

Table 3. Effect of pH on adsorption.

S. No	Concentration (ppm)	pH	Q_e (mg/g)	% R
1	60	1	55.25625	92.09375
2	60	2	58.55625	97.59375
3	60	3	50.30625	83.84375
4	60	4	39.55625	65.92708
5	60	5	28.9875	48.3125
6	60	6	16.74375	27.90625
7	60	7	14.225	23.70833

Effect of contact time

The contact time between the adsorbent and the EBT dye solution plays a crucial role in the adsorption process. Experiments were conducted using 60 ppm dye concentration, 0.1 g of biochar, and pH 2. The adsorption rate was particularly rapid during the first 90 minutes due to the availability of a large number of active sites on the biochar surface. As shown in Table 4, adsorption reached an equilibrium plateau at 120 minutes, indicating that most available sites were occupied. The removal percentage reached approximately 95.31% at this time. Beyond this point, the adsorption rate decreased as fewer open sites remained, surface saturation occurred, and repulsive forces between adsorbed dye molecules developed[56]. The adsorption capacity increased rapidly initially and then gradually leveled off as equilibrium was approached, confirming that 120 minutes is sufficient for achieving maximum adsorption under the tested conditions. This equilibrium time was therefore selected for all subsequent experiments.

Table 4. Effect of contact time on adsorption of EBT Dye.

S. No	Concentration (ppm)	Contact time (min)	Q_t (mg/g)	%R
1	60	0	47.9375	79.89
2	60	30	48.4375	80.7292
3	60	60	55.75	92.916
4	60	90	56.5	94.166
5	60	120	57.1875	95.3125
6	60	150	57.375	95.625
7	60	180	57.5625	95.9375

Thermodynamics studies

Thermodynamic parameters, including entropy (ΔS°), enthalpy (ΔH°), and Gibbs free energy (ΔG°), were calculated at 40, 50, 60, and 70°C using the following equations:

$$\ln KL = \Delta S° R - \Delta H° RT \quad (6)$$

$$\Delta G° = \Delta H° - T\Delta S° \quad (7)$$

The value of ΔG° was obtained by applying the above equation after the values of ΔH° and ΔS° were determined from the slope and intercept of the plot of ln KL vs 1/T (Figure S2). T is the temperature (K), R is the universal gas constant, and KL = qe/Ce is the distribution coefficient (Table S5). Adsorption of EBT is thermodynamically spontaneous and feasible, as indicated by the negative ΔG° value, which becomes less negative as the temperature rises from 40 to 70°C, indicating that the adsorption process is more favorable at higher temperatures. The adsorption is endothermic, as indicated by the positive ΔH° value, and the adsorption increases the randomness at the adsorbent-solution interface, as indicated by the positive ΔS° value.

Adsorption isotherm studies

Adsorption isotherms describe how dye molecules distribute and interact with an adsorbent at equilibrium. They are widely used to evaluate the adsorption behavior of biochar and to determine the maximum adsorption capacity. Isotherms establish the relationship between the residual adsorbate concentration and the adsorption capacity at a constant temperature. For this study, 100 mL of EBT dye solution at an optimum initial concentration of 60 ppm and pH 2.0 was used for the isotherm experiments. A dose of 0.1 g of adsorbent was added to the flasks, which were then agitated at 150 rpm and 25°C for 120 minutes to reach equilibrium. Among several available isotherm models, the Langmuir and Freundlich models were selected for this investigation due to their simplicity and reliability[54,57]. These models provide insights into the adsorption mechanism and surface characteristics of the biochar.

Langmuir adsorption isotherm

The Langmuir adsorption model is based on three fundamental assumptions: the adsorbent has energetically uniform adsorption sites, adsorption occurs as a monolayer, and there is no lateral interaction between adsorbed molecules[58]. The model can be mathematically expressed as:

$$C_e/q_e = \frac{1}{KLqmax} + \frac{C_e}{q_{max}} \quad (8)$$

Where: q_e (mg/g) = amount of dye adsorbed on the solid adsorbent at equilibrium; q_{max} (mg/g) = maximum adsorption capacity of adsorbent; K_L (L/mg) = Langmuir equilibrium constant, related to binding energy; C_e (mg/L) = equilibrium EBT dye concentration. A key feature of the Langmuir isotherm is the dimensionless separation factor, R_L, which indicates the favorability of adsorption. It is defined as follows (Equation 9):

$$R_L = \frac{1}{(1 + K_L C_o)} \quad (9)$$

Where C_o is the initial EBT dye concentration in mg/L. The values of R_L indicate the type of adsorption isotherm: $R_L = 0$; Favorable: $0<R_L<1$; Linear: $R_L = 1$; Unfavorable: $R_L>1$. The maximum adsorption capacity q_{max} and adsorption constant K_L were calculated by graphing $1/Q_e$ vs $1/C_e$ [19] and are presented in Figure S3. With R^2 values of 0.9711, respectively, suggesting the best fit of the adsorption of EBT dye onto the biochar with the Langmuir adsorption process. The Langmuir parameters, summarized in Table S6, show a maximum adsorption capacity of 8.4104 mg/g.

Freundlich adsorption isotherm

The Freundlich isotherm accepts surface heterogeneity and assumes that adsorption occurs at places with differing adsorption energies. The energy of adsorption varies with surface covering[58]. Equation (10) also applies to multilayer adsorption and has the following linear form:

$$\log q_e = \log K_F + \left[\left(\frac{1}{n}\right)(\log C_e)\right] \quad (10)$$

Where K_F (L/mg) denotes the Freundlich constant, and n is the heterogeneity factor. The K_F value is connected to adsorption capacity; the 1/n value is related to adsorption intensity; values of 1/n imply that the isotherm is irreversible: 1/n = 0; Favorable: 0/1; Unfavorable: 1/n > 1 [19]. Figure S4 shows the plot of log Q_e vs log C_e with an R^2 value of 0.392 also, the value of K_F and n were computed from the slope and intercept. Based on the data presented in Table S7 and Figure S4, it can be concluded that the adsorption of EBT dye onto biochar does not fit well with the Freundlich isotherm, suggesting that the adsorption process is better described by the Langmuir model.

Error function analysis

Error function analysis is a key method for evaluating the applicability of experimental data in adsorption studies[58]. In addition to regression coefficients, this study also calculated the nonlinear chi-square test (χ^2) and the root mean square error of the residuals (RMSE). These techniques were used to evaluate the isotherm and adsorption kinetic models. The degree of satisfaction of the model fitting equations increased as the RMSE and chi-square parameter values decreased. The formulas for these two error functions are shown in Equations 11 and 12, respectively.

$$RMSE = \sqrt{\frac{1}{N-2}\sum_{i=1}^{N}\left(q_{e,exp} - q_{e,calc}\right)^2} \quad (11)$$

$$X^2 = \sum_{i=1}^{n}\frac{\left(q_{e,exp} - q_{e,calc}\right)^2}{q_{e,calc}} \quad (12)$$

Where $q_{e,exp}$ (mg/g) represents the adsorption capacity from the batch experiment, n is a numerical value, N is the number of observations in the experimental isotherm, and $q_{e,calc}$ (mg/g) denotes the adsorption capacity calculated from the nonlinear model. Table S6 shows that the Langmuir

isotherm model provides a better fit to the data, with X^2, RMSE, and R^2 values of 1.540, 0.080, and 0.9711, respectively. Thus, the Langmuir model offers a more accurate representation of EBT adsorption on the adsorbent.

Adsorption kinetic studies

Adsorption kinetics play a crucial role in process design, as they determine the rate at which an adsorbent removes contaminants from solution. Kinetic studies also help identify the rate-limiting step and provide insight into the mechanism governing adsorption onto biochar. In this study, 60 ppm EBT dye solutions at pH 2 were treated with 0.1 g of biochar and agitated at 150 rpm for 120 minutes. After the treatment, the samples were filtered, and the residual dye concentration in the clear solution was measured. To analyze the adsorption behavior, three kinetic models were applied: the pseudo-first-order, pseudo-second-order, and and intraparticle diffusion models[22]. These models were used to evaluate the adsorption rate and to infer the mechanism of dye uptake by the biochar.

Pseudo-first-order

The pseudo-first-order equation, which is based on solid capacity, is given by Equation (11):

$$\log (q_e - q_t) = \log q_e - \frac{k_1}{2.303} t \quad (13)$$

Where: q_e is the adsorption capacity at equilibrium (mg/g), q_t is the adsorption capacity at time t (mg/g), and the pseudo-first-order rate constant (min^{-1}) is denoted by k_1[28]. Figure S5 depicts the pseudo-first-order kinetic model by graphing ln (q_e-q_t) versus t. Table S8 and Figure S5 show that the data for EBT dye adsorption are poorly suited to the pseudo-first-order kinetic model, with an R^2 value of 0.7368.

Pseudo-second-order

The pseudo-second-order model is based on the idea that chemisorptions are involved in the rate-limiting phase[58]. The pseudo-second-order rate Equation (12) is written as follows:

$$t/q_t = (1/k_2\, q_e^2) + \left(\frac{1}{q_e} t\right) (14)$$

Where, q_e is the maximal adsorption capacity (mg/g), k_2 is the pseudo-second-order equation rate constant (g/mg.min), and q_t is the quantity of dye adsorbed per unit mass of adsorbent (mg/g)[28]. Figure S6 shows a plot of t/q_t vs t for the pseudo-second-order kinetic model. The slope and intercept may be used to calculate all of the adsorption kinetic parameters. The data in Table S9 showed that EBT dye adsorption suited the second-order kinetic model. Furthermore, in the second-order kinetic model for EBT dye, the differences between Q_t predicted 58.47953 mg/g and Q_t experimental 57.1875 mg/g are less. The adsorption of EBT by Cladophora *golmerata* biochar may be chemisorption, based on the data's fit to the second-order kinetic model. The pseudo-second-order model indicates that chemisorption is the rate-determining step, involving electron sharing or exchange between the adsorbent and adsorbate. The functional groups present on the biochar surface further support this explanation, as these functional groups can chemically interact with dye molecules.

Intraparticle diffusion models

The adsorption data was also analyzed by intra-particle diffusion kinetic model, which is represented by following equation:

$$q_t = K_i t^{1/2} + C (15)$$

Where C is the constant related to the thickness of the boundary layer (mg/g), K_i is the intraparticle diffusion rate constant (mg/g $min^{1/2}$).

The intraparticle diffusion curve (the relationship between qt and $t^{1/2}$) exhibits a multilinear region, indicating that the adsorption process proceeds in multiple stages: the initial stage is rapid external surface

adsorption, followed by a slow intraparticle diffusion stage. The curve does not pass through the origin, indicating that intraparticle diffusion is not the only rate-determining step; boundary layer diffusion and chemisorption also participate in the entire adsorption process.

Comparison of adsorption capacities of several adsorbents

Table 5 summarizes the maximum q_m of various low-cost bio-based adsorbents for EBT. Among the listed materials, biochar derived from *Cladophora glomerata* exhibited a competitive adsorption capacity (58.56 mg/g), comparable to biochar derived from sweet potato (*Ipomoea batatas*) (59.24 mg/g) and green coffee grounds (58.04 mg/g). Treatment methods such as cold plasma or microwaves improved the adsorption performance of almond shells compared to untreated shells, indicating that surface modification can significantly improve dye removal efficiency. In conclusion, these results highlight the potential of algae and plant-based biochars as highly efficient adsorbents in sustainable wastewater treatment.

Table 5. Comparison of different adsorbents used for MO adsorption.

Adsorbent	Q_m **(mg g^{-1})**	**Reference**
Ipomoea batatas derived biochar	59.242	59
Fucus vesiculosus	24.306	60
Untreated almond shell	6.02	61
Cold plasma-treated almond shell	18.18	61
Microwave-treated almond shell	29.41	61
Green coffee residues	58.04	62
Cladophora glomerata derived biochar	58.55625	This article

Conclusion

This study demonstrates that biochar derived from *Cladophora glomerata* is a highly efficient, low-cost, and sustainable adsorbent for removing EBT from aqueous solutions. Prepared via slow pyrolysis, the biochar exhibits high adsorption efficiency (95.31%) under optimized conditions (0.1 g/100 mL biochar, dye concentration 60 ppm, pH 2, contact time 120 min). Equilibrium data conform to the Langmuir model (R^2 = 0.9711), indicating monolayer adsorption with a maximum adsorption capacity of 8.41 mg/g. Kinetic studies follow a pseudo-second-order kinetic model (R^2 = 0.9992), indicating that chemisorption is the rate-determining step. Compared with other low-cost bio-based adsorbents, *Cladophora* biochar exhibits superior adsorption performance, is environmentally friendly, and aligns with the principles of a circular economy. Future research directions could focus on scaling up production, testing with actual industrial wastewater, and exploring surface modification to further enhance its adsorption capacity and selectivity for different dyes.

Credit author statement

F.A. (Conceptualization, Investigation, Methodology, Data Analysis, Writing – Original Draft); **U.F.** (nvestigation, Methodology, Writing – Original Draft); **K.B.** (Investigation, Methodology, Writing – Original Draft); **M.A.H** (Resource, Writing - Review & Editing); **S.A.** (Investigation, Writing – Original Draft); **S.L.B.** (Investigation, Writing – Original Draft); **S.A.** (Investigation, Writing – Original Draft); **N.M.** (Methodology, Writing – Original Draft); **S.S.** (Methodology, Writing – Original Draft); **M.I.** (Supervision, Methodology, Writing – Original Draft); **T.M.S.A.** (Visualization, Writing – Review & Editing); **A.Y.** (Data Curation, Resources, Validation, Visualization).

Declaration of competing interest

The authors declare that they have no known competing financial and non-financial interests or personal relationships that could have appeared to influence the work reported in this paper.

Funding

The authors extend their appreciation to the Deanship of Research and Graduate Studies at King Khalid University for funding this work through the Large Research Project under grant number RGP2/195/46.

Data availability

The datasets used and/or analyzed during the current study are available from the corresponding author on reasonable request.

References

1. Acioly, T. M. D. S., da Silva, M. F., Barbosa, L. A., Iannacone, J. & Viana, D. C. Levels of potentially toxic and essential elements in water and estimation of human health risks in a river located at the interface of Brazilian savanna and Amazon biomes (Tocantins River). *Toxics* **12**, 444 (2024). https://doi.org/10.3390/toxics12070444.
2. Ge, X., Zhang, Y., Hu, X., Wen, M., & Shi, C. (2025). The role of water during the middle or later periods of Class F fly ash-based geopolymerization. *Cem. and Concr. Compos. 160*, 106045. 10.1016/j.cemconcomp.2025.106045.
3. Shi, L., Li, A., Xu, Y., Yang, H., & Yang, G. (2025). A novel ionic-liquid-supported polythieno [3, 2-b] thiophene coating for headspace solid-phase microextraction of phenolic compounds from environmental water via gas chromatography-mass spectrometry. *Microchim Acta. 192*, 307. 10.1007/s00604-025-07157-2.
4. Li, J., Fan, J., Sun, J., Wang, Z., Lv, K., Qu, Y., ... & Ma, W. (2025). A hyperbranched copolymer as high-temperature and salt-resistance fluid

loss reducer for water-based drilling fluids: preparation, evaluation, and mechanism study. *SPE Journal*, *30*(12), 7347-7363.

5. Kaur, J., Tewari, S., Kaur, A. & Malik, R. Dye and dye-containing hazardous waste in water resource. In *Emerging Contaminants in Water and Wastewater: Sources and Substances*, 179–199 (Springer Nature, Cham, 2025). https://doi.org/10.1007/978-3-031-82579-8_8.
6. Adeleke, A. O., Royahu, C. O., Ahmad, A., Dele-Afolabi, T. T., Alshammari, M. B. & Imteaz, M. A novel oyster shell biocomposite for the efficient adsorptive removal of cadmium and lead from aqueous solution: Synthesis, process optimization, modelling and mechanism studies. *PLoS ONE* **19**, e0294286 (2024).
7. Wang, F., Zhang, J., Hu, J., Wang, H., Zeng, Y., Wang, Y.,... Chen, Z. (2024). Simultaneous suppression of As mobilization and N_2O emission from NH_4^+/As-rich paddy soils by combined nitrate and birnessite amendment. *J. Hazard. Mater.* **465**, 133451. doi: https://doi.org/10.1016/j.jhazmat.2024.133451.
8. Jiang, F., Zhang, Y., Xu, X., Mao, Y., Wang, M., Yang, B.,... Zhang, S. (2025). Application of cysteine with Cu2+ to strengthen Fenton-based treatment of coking wastewater used ferric sludge as a source of iron catalyst: Cl- removal and Fe3+/Fe2+ cycling. *J. Enviro. Chem. Eng*. **13**, 117556. doi: https://doi.org/10.1016/j.jece.2025.117556.
9. Ma, X., Wen, P., Fan, Y., Dong, X., Sun, W., Min, F.,... Xie, J. (2026). Quantitative analysis of high-efficiency dewatering under ultrahigh pressures: Moisture storage state and filter-cake pore structure. *Miner. Eng*. **237**, 109969. doi: https://doi.org/10.1016/j.mineng.2025.109969.
10. Islam, S., Belowar, S., Das, S., Rahamatolla, M. & Datta, S. C. Chemistry of natural and synthetic dye materials with metal mordants in various fabrics for sustainable textile applications: A comprehensive review. *Environ. Sci. Pollut. Res.* 1–30 (2025). https://doi.org/10.1007/s11356-025-37102-y.

11. Barik, D., Rakhi Mol, K. M., Anand, G., Nandamol, P. S., Das, D. & Porel, M. Environmental pollutants such as endocrine disruptors/pesticides/reactive dyes and inorganic toxic compounds metals, radionuclides, and metalloids and their impact on the ecosystem. In *Biotechnology for Environmental Sustainability*, 391–442 (Springer Nature, Singapore, 2025). https://doi.org/10.1007/978-981-97-7221-6_15.
12. Lu, J. Y., Bu, Z. Q., Lei, Y. Q., Wang, D., He, B., Wang, J.,... Huang, W. T. (2024). Facile microwave-assisted synthesis of Sb2O3-CuO nanocomposites for catalytic degradation of p-nitrophenol. *J. Mol. Liq.* **409**, 125503. doi: https://doi.org/10.1016/j.molliq.2024.125503.
13. Qin, X., Cui, H., & Zhou, Q. (2023). Physisorption Behaviors of Organochlorine Pesticides on the InP3 Monolayer from Theoretical Insight. *ACS Omega*. **8**, 32168-32175. doi: 10.1021/acsomega.3c04665
14. Guo, P., Xue, R., Zou, Q., Ma, X., Su, C., Zeng, Z.,... Li, L. (2025). Enhanced Ultramicropore of Biomass-Derived Porous Carbon for Efficient and Low-Energy CO2 Capture: Integration of Adsorption and Solar Desorption. *Energy Environ. Mater*. e70140. doi: https://doi.org/10.1002/eem2.70140.
15. Srivatsav, P., Bhargav, B. S., Shanmugasundaram, V., Arun, J., Gopinath, K. P. & Bhatnagar, A. Biochar as an eco-friendly and economical adsorbent for the removal of colorants (dyes) from aqueous environment: A review. *Water* **12**, 3561 (2020). https://doi.org/10.3390/w12123561.
16. Zhou, A., Wu, Q., Zhang, H., Liu, J., Wang, C., Chi, D., & Zhou, H. (2026). RSM-optimized Mg/Al-LDH biochar composite for enhanced phosphorus removal: Insights into interlayer structure evolution and adsorption mechanism. *J. Environ. Manag*. **401**, 128837. https://doi.org/10.1016/j.jenvman.2026.128837.
17. Yang, C., Zhou, Y., Wang, X., & Zhou, Y. (2026). Sustainable High Thermal Conductivity Composites from Biomass: Bio-Based

Polyimide/Microencapsulated CNTs for Green Thermal Management. *ACS Appl. Polym. Mater*. **8**, 2762-2775. doi: 10.1021/acsapm.5c04260.

18. Lellis, B., Fávaro-Polonio, C. Z., Pamphile, J. A. & Polonio, J. C. Effects of textile dyes on health and the environment and bioremediation potential of living organisms. *Biotechnol. Res. Innov.* **3**, 275–290 (2019). https://doi.org/10.1016/j.biori.2019.09.001.
19. de Oliveira, Z. B., Silva da Costa, D. V., da Silva dos Santos, A. C., da Silva Júnior, A. Q., de Lima Silva, A., de Santana, R. C. F. & da Silva, S. K. R. Synthetic colors in food: A warning for children's health. *Int. J. Environ. Res. Public Health* **21**, 682 (2024). https://doi.org/10.3390/ijerph21060682.
20. Negi, A. Natural dyes and pigments: Sustainable applications and future scope. *Sustain. Chem.* **6**, 23 (2025). https://doi.org/10.3390/suschem6030023.
21. Haghighat, G. A., Sadeghi, S., Saghi, M. H., Ghadiri, S. K., Anastopoulos, I., Giannakoudakis, D. A. & Shams, M. Zeolitic imidazolate frameworks (ZIFs) of various morphologies against eriochrome black-T (EBT): Optimizing the key physicochemical features by process modeling. *Colloids Surf. A Physicochem. Eng. Asp.* **606**, 125391 (2020). https://doi.org/10.1016/j.colsurfa.2020.125391.
22. Bansal, M., Patnala, P. K. & Dugmore, T. Adsorption of Eriochrome Black-T (EBT) using tea waste as a low cost adsorbent by batch studies: A green approach for dye effluent treatments. *Curr. Res. Green Sustain. Chem.* **3**, 100036 (2020). https://doi.org/10.1016/j.crgsc.2020.100036.
23. Elijah, O. C. & Nwabanne, J. T. Adsorption studies on the removal of Eriochrome Black-T from aqueous solution using Nteje clay. *SOP Trans. Appl. Chem.* **1**, 14–25 (2014).
24. Sharifpour, E., Khafri, H. Z., Ghaedi, M., Asfaram, A. & Jannesar, R. Isotherms and kinetic study of ultrasound-assisted adsorption of malachite green and Pb^{2+} ions from aqueous samples by copper sulfide nanorods loaded on activated carbon: Experimental design optimization.

Ultrason. Sonochem. **40**, 373–382 (2018). https://doi.org/10.1016/j.ultsonch.2017.07.030.

25. Kaur, Y., Jasrotia, T., Kumar, R., Chaudhary, G. R. & Chaudhary, S. Adsorptive removal of Eriochrome Black T (EBT) dye by using surface active low cost zinc oxide nanoparticles: A comparative overview. *Chemosphere* **278**, 130366 (2021). https://doi.org/10.1016/j.chemosphere.2021.130366.
26. Fan, J., Zhang, X., He, N., Song, F., & Wang, X. (2025). Investigation on novel deep eutectic solvents with high carbon dioxide adsorption performance. *J. Environ. Chem. Eng.* ***13***, 117870.
27. de Luna, M. D. G., Flores, E. D., Genuino, D. A. D., Futalan, C. M. & Wan, M. W. Adsorption of Eriochrome Black T (EBT) dye using activated carbon prepared from waste rice hulls—Optimization, isotherm and kinetic studies. *J. Taiwan Inst. Chem. Eng.* **44**, 646–653 (2013). https://doi.org/10.1016/j.jtice.2013.01.010.
28. Aziz, E. K., Abdelmajid, R., Rachid, L. M. & Mohammadine, E. H. Adsorptive removal of anionic dye from aqueous solutions using powdered and calcined vegetable wastes as low-cost adsorbent. *Arab J. Basic Appl. Sci.* **25**, 93–102 (2018). https://doi.org/10.1080/25765299.2018.1517861.
29. Boumchita, S., Lahrichi, A., Benjelloun, Y., Lairini, S., Nenov, V. & Zerrouq, F. Application of peanut shell as a low-cost adsorbent for the removal of anionic dye from aqueous solutions. *J. Mater. Environ. Sci.* **8**, 2353–2364 (2017).
30. Devi, P. & Saroha, A. K. Effect of pyrolysis temperature on polycyclic aromatic hydrocarbons toxicity and sorption behaviour of biochars prepared by pyrolysis of paper mill effluent treatment plant sludge. *Bioresour. Technol.* **192**, 312–320 (2015). https://doi.org/10.1016/j.biortech.2015.05.084.
31. Oliveira, F. R., Patel, A. K., Jaisi, D. P., Adhikari, S., Lu, H. & Khanal, S. K. Environmental application of biochar: Current status and

perspectives. *Bioresour. Technol.* **246**, 110–122 (2017). https://doi.org/10.1016/j.biortech.2017.08.122.

32. Wang, J. & Wang, S. Preparation, modification and environmental application of biochar: A review. *J. Clean. Prod.* **227**, 1002–1022 (2019). https://doi.org/10.1016/j.jclepro.2019.04.282.
33. Ahmad, W., Zakir, M., Khan, N., Muhammad, T., Khan, R., da Silva Acioly, T. M. & Ibáñez-Arancibia, E. Sustainable removal of hydrocarbon contaminants in refinery wastewater with metal-organic frameworks. *Chem. Ecol.* **41**, 1187–1204 (2025). https://doi.org/10.1080/02757540.2025.2533269.
34. Ren, Y. S., Tynybekov, B., Nurmahanova, A., Ibragimov, T., Kurmanbay, U., Nazarbekova, S. & Machado da Silva Acioly, T. Eucalyptus wood waste biochar: a green solution for fluoranthene contamination in wastewater. *Int. J. Environ. Health Res.* 1–14 (2025). https://doi.org/10.1080/09603123.2025.2483976.
35. Nautiyal, P., Subramanian, K. A. & Dastidar, M. G. Adsorptive removal of dye using biochar derived from residual algae after in-situ transesterification: Alternate use of waste of biodiesel industry. *J. Environ. Manage.* **182**, 187–197 (2016). https://doi.org/10.1016/j.jenvman.2016.07.063.
36. Michalak, I., Baśladyńska, S., Mokrzycki, J. & Rutkowski, P. Biochar from a freshwater macroalga as a potential biosorbent for wastewater treatment. *Water* **11**, 1390 (2019). https://doi.org/10.3390/w11071390.
37. Son, E. B., Poo, K. M., Chang, J. S. & Chae, K. J. Heavy metal removal from aqueous solutions using engineered magnetic biochars derived from waste marine macro-algal biomass. *Sci. Total Environ.* **615**, 161–168 (2018). https://doi.org/10.1016/j.scitotenv.2017.09.171.
38. Zhou, Y., Zhang, H., Cai, L., Guo, J., Wang, Y., Ji, L. & Song, W. Preparation and characterization of macroalgae biochar nanomaterials with highly efficient adsorption and photodegradation ability. *Materials* **11**, 1709 (2018). https://doi.org/10.3390/ma11091709.

39. De Bhowmick, G., Sarmah, A. K. & Sen, R. Production and characterization of a value added biochar mix using seaweed, rice husk and pine sawdust: A parametric study. *J. Clean. Prod.* **200**, 641–656 (2018). https://doi.org/10.1016/j.jclepro.2018.08.002.

40. Wang, H., Zhang, M. & Lv, Q. Removal efficiency and mechanism of Cr(VI) from aqueous solution by maize straw biochars derived at different pyrolysis temperatures. *Water* **11**, 781 (2019). https://doi.org/10.3390/w11040781.

41. Mihranyan, A. Cellulose from cladophorales green algae: From environmental problem to high-tech composite materials. *J. Appl. Polym. Sci.* **119**, 2449–2460 (2011). https://doi.org/10.1002/app.32959.

42. Chaiwong, K., Kiatsiriroat, T., Vorayos, N. & Thararax, C. Biochar production from freshwater algae by slow pyrolysis. *Maejo Int. J. Sci. Technol.* **6**, 186 (2012).

43. Poo, K. M., Son, E. B., Chang, J. S., Ren, X., Choi, Y. J. & Chae, K. J. Biochars derived from wasted marine macro-algae (Saccharina japonica and Sargassum fusiforme) and their potential for heavy metal removal in aqueous solution. *J. Environ. Manage.* **206**, 364–372 (2018). https://doi.org/10.1016/j.jenvman.2017.10.056.

44. Leng, L., Yuan, X., Huang, H., Shao, J., Wang, H., Chen, X. & Zeng, G. Bio-char derived from sewage sludge by liquefaction: Characterization and application for dye adsorption. *Appl. Surf. Sci.* **346**, 223–231 (2015). https://doi.org/10.1016/j.apsusc.2015.04.014.

45. Michalak, I., Mironiuk, M. & Marycz, K. A comprehensive analysis of biosorption of metal ions by macroalgae using ICP-OES, SEM-EDX and FTIR techniques. *PLoS ONE* **13**, e0205590 (2018). https://doi.org/10.1371/journal.pone.0205590.

46. Ungureanu, E., Tofanica, B. M., Ulea, E., Ungureanu, O. C., Fortună, M. E., Rotaru, R. & Popa, V. I. Valorization of agro-industrial lignin as a functional polymer for sustainable wastewater treatment. *Polymers* **17**, 2263 (2025). https://doi.org/10.3390/polym17162263.

47. Han, Y. J., Chung, D., Nakabayashi, K., Chung, J. D., Miyawaki, J. & Yoon, S. H. Effect of heat pre-treatment conditions on the electrochemical properties of mangrove wood-derived hard carbon as an effective anode material for lithium-ion batteries. *Electrochim. Acta* **213**, 432–438 (2016). https://doi.org/10.1016/j.electacta.2016.07.138.

48. Bird, M. I., Wurster, C. M., de Paula Silva, P. H., Bass, A. M. & De Nys, R. Algal biochar–production and properties. *Bioresour. Technol.* **102**, 1886–1891 (2011). https://doi.org/10.1016/j.biortech.2010.07.106.

49. Tomczyk, A., Sokołowska, Z. & Boguta, P. Biochar physicochemical properties: Pyrolysis temperature and feedstock kind effects. *Rev. Environ. Sci. Biotechnol.* **19**, 191–215 (2020). https://doi.org/10.1007/s11157-020-09523-3.

50. Greenwood, J. L., Clason, T. A., Lowe, R. L. & Belanger, S. E. Examination of endopelic and epilithic algal community structure employing scanning electron microscopy. *Freshw. Biol.* **41**, 821–828 (1999). https://doi.org/10.1046/j.1365-2427.1999.00420.x.

51. Liu, H., Chen, Y., Yang, H., Gentili, F. G., Söderlind, U., Wang, X. & Chen, H. Hydrothermal carbonization of natural microalgae containing a high ash content. *Fuel* **249**, 441–448 (2019). https://doi.org/10.1016/j.fuel.2019.03.004.

52. Salimi, P., Javadian, S., Norouzi, O. & Gharibi, H. Turning an environmental problem into an opportunity: Potential use of biochar derived from a harmful marine biomass named Cladophora glomerata as anode electrode for Li-ion batteries. *Environ. Sci. Pollut. Res.* **24**, 27974–27984 (2017). https://doi.org/10.1007/s11356-017-0181-1.

53. Shah, Z., Badshah, S. L., Alves, J. L. F., da Silva, J. C. G. & Iqbal, A. Pyrolysis kinetics and thermodynamic parameters of macroalgae Cladophora glomerata based on multi-step devolatilization to assess its bioenergy potential. *Biomass Convers. Biorefin.* 1–14 (2022). https://doi.org/10.1007/s13399-022-02556-4.

54. Abd, I. N. & Mohammed-Ridha, M. J. Tetracycline antibiotic removal from aqueous solution using cladophora and spirulina algae biomass. *Iraqi J. Agric. Sci.* **52**, 336–347 (2021). https://doi.org/10.36103/ijas.v52i2.1295.

55. Tao, X., Liu, S., He, H., Lv, L., Sun, L., Zhang, P. & Zhang, G. Machine learning-driven optimization of Lanthanum-based adsorbents for enhancing phosphate adsorption from water. *J. Environ. Chem. Eng.* 117900 (2025). https://doi.org/10.1016/j.jece.2025.117900.

56. Parsa, M., Nourani, M., Baghdadi, M., Hosseinzadeh, M. & Pejman, M. Biochars derived from marine macroalgae as a mesoporous by-product of hydrothermal liquefaction process: Characterization and application in wastewater treatment. *J. Water Process Eng.* **32**, 100942 (2019). https://doi.org/10.1016/j.jwpe.2019.100942.

57. Ahmed, H. R., Kayani, K. F., Ealias, A. M. & Aziz, K. H. H. A comprehensive review of forty adsorption isotherm models: An in-depth analysis of ten statistical error measures. *Water Air Soil Pollut.* **236**, 346 (2025). https://doi.org/10.1007/s11270-025-07982-4.

58. Ren, Y. S., He, Q., Liao, W., Liao, Y., Zhan, Z., Xu, J. & Ilyas, M. Sustainable adsorbent: Activated carbon from waste styrofoam for efficient aluminum removal. *Microsc. Res. Tech.* **88**, 1044–1054 (2025).

59. Akpomie, K. G. & Conradie, J. Ultrasonic-assisted adsorption of eriochrome black T and celestine blue dyes onto Ipomoea batatas-derived biochar. *Int. J. Environ. Anal. Chem.* **103**, 8670–8688 (2023).

60. Lebron, Y. A. R., Moreira, V. R. & de Souza Santos, L. V. Biosorption of methylene blue and eriochrome black T onto the brown macroalgae Fucus vesiculosus: Equilibrium, kinetics, thermodynamics and optimization. *Environ. Technol.* **42**, 279–297 (2021).

61. Şahin, Ö., Saka, C. & Kutluay, S. Cold plasma and microwave radiation applications on almond shell surface and its effects on the adsorption of Eriochrome Black T. *J. Ind. Eng. Chem.* **19**, 1617–1623 (2013).

62. Manzar, M. S., Zubair, M., Khan, N. A., Husain Khan, A., Baig, U., Aziz, M. A. & Abdel-Magid, H. I. Adsorption behaviour of green coffee residues for decolourization of hazardous Congo Red and Eriochrome Black T dyes from aqueous solutions. *Int. J. Environ. Anal. Chem.* **102**, 6405–6421 (2022).